REPORT DOCUMENTATION PAGE

Form Approved
OMB No. 0704-0188

1. REPORT DATE *(DD-MM-YYYY)*	**2. REPORT TYPE**	**3. DATES COVERED** *(From - To)*
October 2013	Open Literature	

4. TITLE AND SUBTITLE
Structural, morphological and functional correlates of corneal endothelial toxicity following corneal exposure to sulfur mustard vapor

5a. CONTRACT NUMBER

5b. GRANT NUMBER

5c. PROGRAM ELEMENT NUMBER

6. AUTHOR(S)
McNutt, PM., Tuznik, K., Nelson, M., Adkins, A., Lyman, M., Glotfelty, E., Hughes, J., Hamilton, T.

5d. PROJECT NUMBER

5e. TASK NUMBER

5f. WORK UNIT NUMBER

7. PERFORMING ORGANIZATION NAME(S) AND ADDRESS(ES)

US Army Medical Research Institute of Chemical Defense
ATTN: MCMR-CDR-C
3100 Ricketts Point Road
Aberdeen Proving Ground, MD 21010-5400

8. PERFORMING ORGANIZATION REPORT NUMBER

USAMRICD-P13-015

9. SPONSORING / MONITORING AGENCY NAME(S) AND ADDRESS(ES)
Defense Threat Reduction Agency
8725 John J. Kingman Road STOP 6201
Fort Belvoir, VA 22060-6201

10. SPONSOR/MONITOR'S ACRONYM(S)

11. SPONSOR/MONITOR'S REPORT NUMBER(S)

12. DISTRIBUTION / AVAILABILITY STATEMENT

Approved for public release; distribution unlimited

13. SUPPLEMENTARY NOTES
Published in Investigative Ophthalmology & Visual Science, 54(10), 6735–6744, 2013. This research was supported by the Defense Threat Reduction Agency- Joint Science and Technology Office, Medical S&T Division (grant CBM.CUTOC. 01.12.RC.006).

14. ABSTRACT
See reprint.

15. SUBJECT TERMS
sulfur mustard, corneal endothelial cells, mustard gas, mustard gas keratopathy, corneal edema

16. SECURITY CLASSIFICATION OF:			**17. LIMITATION OF ABSTRACT**	**18. NUMBER OF PAGES**	**19a. NAME OF RESPONSIBLE PERSON**
a. REPORT	**b. ABSTRACT**	**c. THIS PAGE**			Patrick McNutt
UNCLASSIFIED	UNCLASSIFIED	UNCLASSIFIED	UNLIMITED	10	**19b. TELEPHONE NUMBER** *(include area code)* 410-436-8044

Structural, Morphological, and Functional Correlates of Corneal Endothelial Toxicity Following Corneal Exposure to Sulfur Mustard Vapor

Patrick McNutt, Kaylie Tuznik, Marian Nelson, Angie Adkins, Megan Lyman, Elliot Glotfelty, James Hughes, and Tracey Hamilton

United States Army Medical Research Institute of Chemical Defense, Aberdeen Proving Grounds, Maryland

Correspondence: Patrick McNutt, United States Army Medical Research Institute of Chemical Defense, Aberdeen Proving Grounds, MD 21010; Patrick.mcnutt@us.army.mil.

Submitted: May 13, 2013
Accepted: September 7, 2013

Citation: McNutt P, Tuznik K, Nelson M, et al. Structural, morphological, and functional correlates of corneal endothelial toxicity following corneal exposure to sulfur mustard vapor. *Invest Ophthalmol Vis Sci*. 2013;54:6735–6744. DOI:10.1167/iovs.13-12402

Purpose. Sulfur mustard (SM) is a highly reactive vesicant that causes severe ocular injuries. Following exposure to moderate or high doses, a subset of victims develops a chronic injury known as mustard gas keratopathy (MGK) involving a keratitis of unknown etiopathogenesis with secondary keratopathies such as persistent epithelial lesions, corneal neovascularization, and progressive corneal degeneration. This study was designed to determine whether SM exposure evokes acute endothelial toxicity and to determine whether endothelial pathologies were specifically observed in MGK corneas as opposed to healed corneas.

Methods. Corneas of New Zealand white rabbits were exposed to SM vapor, and the corneal endothelium was evaluated at 1 day and 8 weeks using scanning electron microscopy (SEM), transmission electron microscopy (TEM), in vivo confocal microscopy (IVM), and fluorescent microscopy. Barrier function was measured by uptake of a fluorescent dye injected into the anterior chamber.

Results. A centripetal endothelial injury at 1 day was observed by SEM, TEM, IVM, and fluorescent microscopy. In vivo confocal microscopy revealed additional cytotoxicity between 1 and 13 days. In contrast to healed corneas, which appeared similar to sham-exposed naive eyes at 8 weeks, MGK corneas exhibited significant evidence of continued pathological changes in the endothelium.

Conclusions. Endothelial toxicity occurs at the right time and with the appropriate pathophysiology to contribute to MGK. Based on these findings, we propose a model that explains the relationships among SM dose, the biphasic progression, and the various clinical trajectories of corneal SM injury and that provides a mechanism for temporal variations in MGK onset. Finally, we discuss the implications for the management of SM casualties.

Keywords: sulfur mustard, corneal endothelial cells, mustard gas, mustard gas keratopathy, corneal edema

Sulfur mustard (SM) is a vesicating chemical warfare agent that rapidly alkylates biological material, causing cytotoxicity and eliciting a proinflammatory response.[1] The eyes are the most susceptible tissue to SM, and even brief exposures can cause debilitating ocular injuries. While mild corneal exposures often resolve uneventfully, moderate or severe exposures can develop into a chronic injury known as mustard gas keratopathy (MGK), which may appear immediately (chronic form) or after a clinically quiescent period ranging from 0.5 to 40 years (delayed-onset form).[1–3] Although the relationship between the chronic and delayed-onset forms of MGK is unclear, both involve a chronic noninfectious keratitis with secondary keratopathies such as persistent epithelial lesions, corneal neovascularization, and progressive corneal degeneration.[4,5] Host corneal tissue removed during surgical interventions exhibits signs of chronic inflammation, suggesting a persistent injury that is beyond the healing capacity of the cornea.[2,6] However, the pathogenic mechanisms of MGK are currently unknown.

Without a clear understanding of the etiopathogenesis of the chronic SM injury, treatments have been mostly palliative in nature. Surgical interventions such as corneal keratoplasty have had mixed outcomes, with successes occurring in mild cases of MGK.[2,6] In animal models of MGK, the prompt administration of anti-inflammatory agents and protease inhibitors delayed the onset of chronic symptoms; however, MGK symptoms subsequently developed on cessation of therapy, suggesting that treatments which fail to resolve the underlying pathologies are unlikely to prevent the onset of MGK.[7–10]

To better understand the pathogenesis of MGK, we have developed a rabbit ocular exposure model based on local application of SM vapor to the corneal surface and have shown that this model exhibits dose-dependent, multiphasic corneal injuries with sequelae similar to those observed in humans.[11,12] Exposed corneas develop an acute lesion within 1 day characterized by vesication of the corneal epithelium, stromal keratocytosis, and corneal edema. The anterior cornea exhibits a robust healing response, regenerating an intact stratified epithelium within 1 week. Grossly, corneas appear to be healing from 1 to 2 weeks (the quiescent phase), with few clinical symptoms other than lingering edema. Resolving corneas subsequently undergo a decrease in corneal thickness,

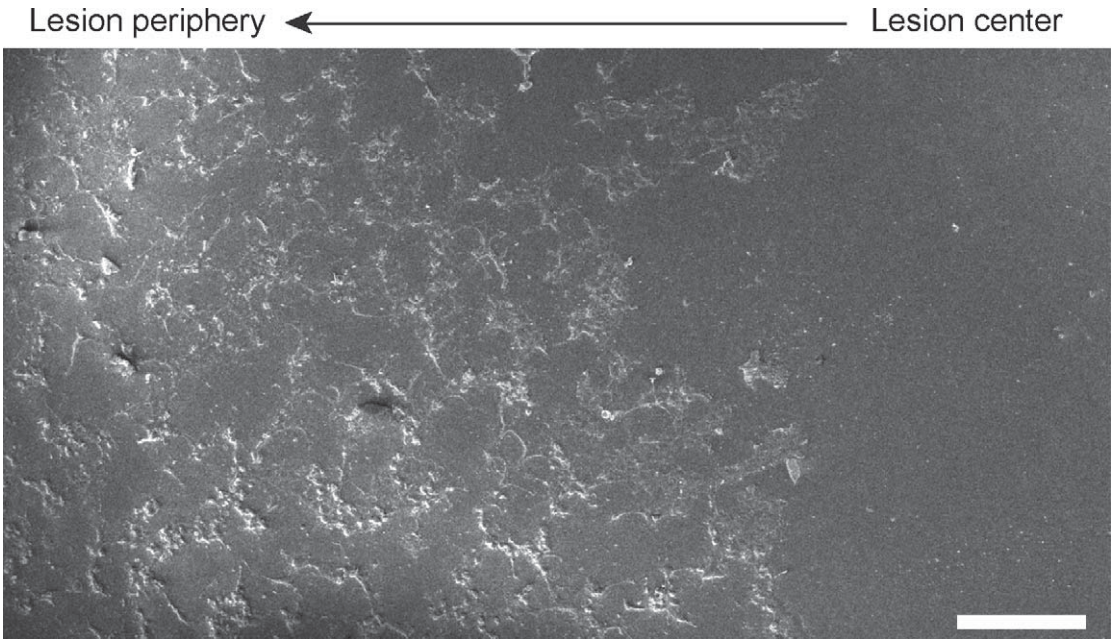

Figure 1. Representative ×70 SEM demonstrating the centripetal nature of the endothelial SM injury, with a central denuded region and increased CEC retention at the injury penumbra. *Scale bar*: 100 μm.

reaching baseline levels by 6 weeks.[11,13] In contrast, MGK corneas develop a persistent edema as soon as 3 weeks with recurring epithelial toxicity, basement membrane zone degeneration, and redundant deposition of basement membrane components following cyclical attempts to regenerate the epithelium.[14] Secondary pathologies such as epithelial bullae, neovascularization, and limbal stem cell niche dysfunction subsequently appear, further interfering with stable repair of the ocular surface.[11,13] The distinct pathophysiology of MGK revealed in these studies suggests the involvement of injury mechanisms that operate on different time scales and in different corneal compartments than during the acute injury.[14] However, these findings did not reveal a pathology that was expressed in a spatiotemporal fashion to be responsible for the pathogenesis of MGK.

The first clinical symptom of MGK onset is a sustained edema, raising the possibility that chronic edema is associated with the pathogenesis of MGK.[14] In rabbits, edema is localized in the posterior central cornea at 2 weeks, immediately before MGK onset. Given the anisotropic hydrodynamics of the stroma, this suggests that the origin of edema is also centrally located.[15] Because (1) the corneal epithelium regenerates an intact epithelial cap by 5 days after exposure that remains intact until after MGK onset and (2) neovascularization does not extend to the central cornea until approximately 8 weeks, the most likely source of corneal edema is dysfunction of the corneal endothelium.[11–14] Hypothesizing that the acute or chronic SM injury may involve endothelial toxicity, we evaluated the structure and function of the corneal endothelium during the acute SM injury and in resolved versus MGK corneas at 8 weeks.

Methods

Ethics Statement and Disclaimers

The experimental protocol was approved by the Animal Care and Use Committee at the United States Army Medical Research Institute of Chemical Defense (United States Department of Agriculture certificate No. 51-F-0006). All procedures were in compliance with the ARVO Statement for the Use of Animals in Ophthalmic and Vision Research and were conducted in accord with the principles stated in the Guide for the Care and Use of Laboratory Animals and the Animal Welfare Act of 1966 (Pub L No. 89-544), as amended.

Animals

Sixty female New Zealand white rabbits (Charles River Laboratories, Germantown, MD) weighing 2.0 to 2.5 kg were housed individually. Rabbits were provided a standard diet with regular enrichment and water ad libitum. At either 1 day or 8 weeks after SM exposure, rabbits were anesthetized with an intramuscular administration of 15 mg/kg of ketamine and 7 mg/kg of xylazine and euthanized by cardiac injection of sodium pentobarbital. Globes were enucleated and corneas processed as described below.

Exposure Procedures

Rabbits were exposed in cohorts of 8 to 16 animals during a 4-month period. One day before exposure, a 4-in^2 region on each rabbit's back was clipped, and a fentanyl patch (25 μg/h) was placed anterior to the scapula. On the day of exposure, rabbits were anesthetized with an intramuscular administration of 15 mg/kg of ketamine and 7 mg/kg of xylazine, and physiological parameters were recorded. The right corneas of anesthetized rabbits were exposed to SM vapor for 2.5 min using a vapor cup delivery system as previously described.[11,12] Two minutes after exposure, exposed eyes were gently rinsed with 10 mL sterile saline to flush residual agent. Rabbits were returned to cages and provided food and water ad libitum. Fentanyl patches were replaced after 72 hours to manage discomfort through 6 days after the exposure and applied liberally thereafter as needed. Animals were monitored daily for signs of pain and distress. Corneal injury was clinically evaluated on a regular basis using pachymetry, fluorescein exclusion assays, and slitlamp evaluations.

Investigative Ophthalmology & Visual Science

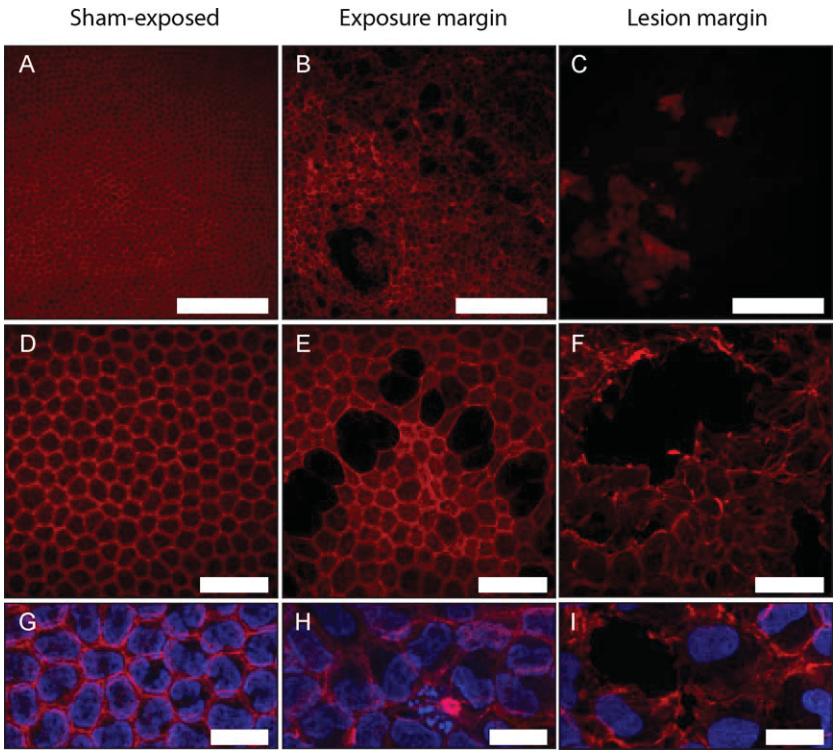

Figure 2. Fluorescent microscopy of changes in endothelial cell morphology 24 hours after corneal exposure to SM vapor. Sham-exposed CECs (**A**, **D**, **G**) are compared with CECs at the margins of the exposure region (**B**, **E**, **H**) and at the edges of the central lesion (**C**, **F**, **I**). (**A–C**) ×20 Images of F-actin distribution. *Scale bars*: 200 μm. (**D–F**) ×63 Images of F-actin distribution. *Scale bars*: 50 μm. (**G–I**) ×100 Images of F-actin distribution and nuclear morphologies. Note the nuclear overlap and fragmentation in (**H**), indicative of overlapping cell bodies, and the swollen nuclei in (**I**), suggestive of ongoing cell death. *Scale bars*: 20 μm.

Whole-Mount Fluorescent Microscopy

The cornea and lens ($n = 6$ each, sham and exposed) were excised from the globe using iridectomy scissors and immersion fixed for 15 minutes in 4% paraformaldehyde (Sigma-Aldrich Corp., St. Louis, MO) in PBS. Fixed corneas were washed thoroughly in PBS with 0.1% saponin (PBSS; Sigma-Aldrich Corp.) and then blocked overnight at 4°C in PBSS plus 3% BSA (Sigma-Aldrich Corp.) in a 12-well dish. Corneas were incubated with 330 nM phalloidin–Alexa 555 (Invitrogen, Carlsbad, CA) in PBSS for 20 minutes, washed three times with PBSS, and mounted on a slide with coverslip using Prolong DAPI Gold (Invitrogen). After drying, corneas were imaged using a Zeiss LSM 700 confocal microscope and analyzed with Zen 2009 (Carl Zeiss Microscopy, LLC, Thornwood, NY).

Electron Microscopy

Following enucleation, buffered 2.5% glutaraldehyde was injected into the aqueous humor via the cornea at the limbal margin. A venting needle was inserted into the cornea directly opposite the injection site to alleviate injection pressure. Globes were then immersed in 2.5% glutaraldehyde for 1 day. Corneal caps were excised using iridectomy scissors, postfixed in buffered 1% osmium tetroxide, dehydrated in graded ethanol, and embedded in Poly/Bed 812 embedding resin (Polysciences, Inc., Warrington, PA) for transmission electron microscopy (TEM) analysis. Ninety-nanometer-thick sections were mounted on copper mesh grids and counterstained with uranyl acetate and lead citrate. Corneal sections were imaged using a JEM-1230 transmission electron microscope (JEOL Ltd., Tokyo, Japan). For scanning electron microscopy (SEM), corneas were dissected from the globe using iridectomy scissors, and the central cornea was removed using an 8-mm biopsy punch. Tissue punches were postfixed in buffered 1% osmium tetroxide, dehydrated in graded ethanol, and critical point dried. Mounted samples were ion beam coated using gold/palladium and imaged using an 7401F field emission scanning electron microscope (JEOL Ltd.). Observations of sequelae in at least 75% of corneas were considered to be genuine. Measurements of corneal size were performed by measuring the longest axis of 150 cells per cornea, three corneas per condition.

Measurements of Endothelial Permeability

Rabbits were euthanized 24 hours after exposure. Five minutes after euthanasia, 20 μL of a 0.1 mg/mL solution of AlexaFluor 488 (Life Technologies, Carlsbad, CA) dissolved in PBS (pH 7.4) was injected into the anterior chamber through a 30-gauge needle using a 100-μL Hamilton glass syringe (Hamilton Company, Reno, NV). The sham-exposed contralateral eye was injected first, followed by the exposed eye. After 10 minutes, corneas were excised and washed three times for 1 minute in 10 mL PBS. Corneas were transferred to 14-mL round-bottom tubes (Becton Dickinson, Franklin Lakes, NJ) with 100 μL PBS and incubated on ice in the dark with gentle agitation. After 30 minutes, supernatant was diluted 1:5 in PBS and analyzed for fluorescence on a Synergy MX fluorophotometer (Biotek, Winooski, VT) using an excitation wavelength of 488 ± 10 nm, emission wavelength of 524 ± 10 nm, and a gain of 50. Representative corneas were imaged with a blue

Investigative Ophthalmology & Visual Science

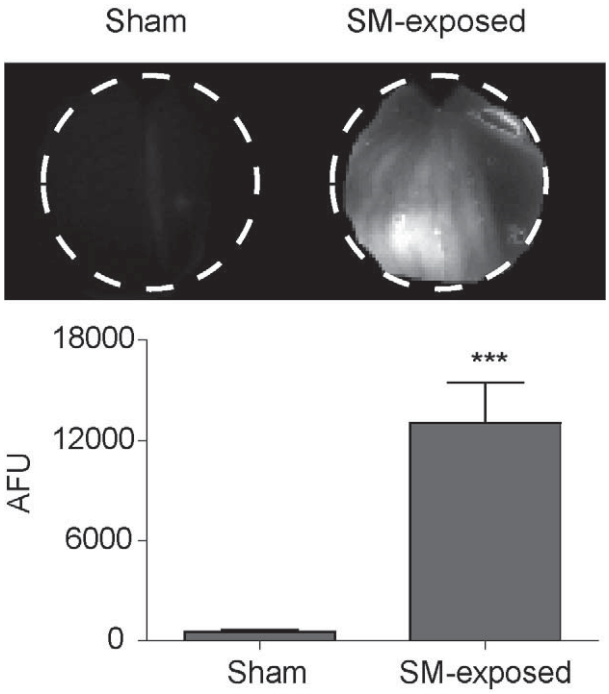

FIGURE 3. Corneas exhibit increased endothelial permeability 24 hours after vapor SM exposure. *Top*: Representative fluorescent images of control and SM-exposed corneas demonstrating increased uptake of AlexaFluor 488 from the aqueous humor. *Bottom*: The average fluorescent dye in corneas harvested from SM-exposed versus contralateral control eyes ($n = 8$ each). *Error bars* denote ±1 SD. $^{***}P < 0.001$.

diode and FITC filter set in a Versadoc MP 4000 (Bio-Rad Laboratories, Hercules, CA).

In Vivo Confocal Microscopy of Rabbit Eyes

For in vivo confocal microscopy (IVM), 26 rabbits were anesthetized with intramuscular administration of 15 mg/kg of ketamine and 7 mg/kg of xylazine and wrapped in a canvas Snuggle (Lomir Biomedical, Inc., Malone, NY) for secure handling. Corneas were imaged before exposure at 1 and 13 days using a Confoscan IV (Nidek, Inc., Fremont, CA) with an ×40 objective in gel immersion mode and a viscous contact solution (GenTeal Gel; Novartis Ophthalmics, East Hanover, NJ). To facilitate use with rabbits, the Confoscan IV (Nidek, Inc.) was modified by removing the headrest and taping the chinrest down. Following imaging, rabbits were returned to individual caging and observed until sternal. At least three attempts were made to image each cornea. Rabbits that could not be imaged at 1 day were excluded from subsequent analysis to minimize unnecessary handling. Corneal cell density was determined from images of the endothelium using automated cell counting software (NAVIS; Nidek, Inc.) and verified by manual enumeration of nuclei.

Statistical Comparisons

Prism version 5.04 (GraphPad Software, Inc., La Jolla, CA) was used for statistical comparisons and graphing. For binary comparisons of means, Student's *t*-test was used. Multiple comparisons were performed using one-way ANOVA (repeated-measures ANOVA for IVM data), and significance was determined by comparison with control values using Dunnett's multiple comparisons test. Unless otherwise stated, all data are presented as the mean ± 1 SD. Markers of statistical significance are presented in the figure legends.

RESULTS

SM Vapor Exposure Causes Corneal Endothelial Cell Vesication Within 24 Hours

Corneas visualized at ×70 by SEM 24 hours after SM exposure exhibited a centripetal injury, with extensive loss of corneal endothelial cells (CECs) in the central cornea and increased retention toward the exposure margins (Fig. 1). The diameter of the acellular central lesion varied from 0.5 to 1 mm, with an additional 1-mm to 2-mm lesion periphery characterized by the patchy retention of cells. The effect of vapor SM exposure on endothelial cell loss was evaluated at higher resolution using fluorescent microscopy imaging of F-actin distribution.[16] In sham-exposed corneas, a regular pattern of polygonal cells was observed, with predominantly hexagonal shape and peripheral accumulation of actin (Figs. 2A, 2D). Following SM exposure, corneas exhibited a spectrum of injuries ranging from gross endothelial sloughing to scattered loss of CECs (Figs. 2B, 2C). In areas with significant cell loss, the remaining CECs were often highly disorganized and enlarged (Figs. 2E, 2F). Nuclear staining indicated the presence of nuclear fragmentation and swelling, characteristic of terminally injured CECs (Figs. 2G–I).

SM Exposure Results in Increased Endothelial Permeability In Vivo at 24 Hours

The ability of the endothelium to maintain corneal deturgescence depends on osmotic pump activity and the integrity of the CEC monolayer. To determine whether SM exposure results in the acute disruption of endothelial function, stromal absorption of a fluorescent dye injected into the aqueous humor was quantified 1 day after exposure. The SM-exposed corneas absorbed 20-fold more fluorophore than control corneas in a 10-minute period ($n = 8$, $P < 0.001$) (Fig. 3), confirming that SM exposure increased endothelial permeability.

SM Induces Changes in Endothelial Structure and Morphology at 24 Hours

To obtain a more comprehensive overview of SM-induced changes in the corneal endothelium, the fine structure of the posterior cornea was evaluated by electron microscopy. En face scanning electron micrographs of sham-exposed corneas revealed a continuous layer of polygonal cells of regular shape and size, with interdigitated borders, apical microvilli, and infrequent cilia (Fig. 4A). Within 24 hours of exposure, all corneal endothelia exhibited evidence of an acute lesion, with extensive central CEC loss and more diffuse vesication in the exposure penumbra. The CECs within the exposed region displayed two general morphologies, namely, enlarged (highly attenuated) polymorphic cells and rounded or spindle-shaped cells (Fig. 4B). Most CECs exhibited atypical apical membrane morphologies and lacked cell-to-cell interdigitations (Figs. 4B, 4C). In regions of CEC vesication, denuded Descemet's membrane (DM) was covered by a complex arbor of CEC lamellipodia and filopodia (Fig. 4D). The TEM imaging of corneal cross-sections confirmed the centripetal injury pattern, with CEC morphology progressively normalizing toward the injury margin (Fig. 5). Denuded DM near the central lesion was infiltrated by extensively arborized cellular processes. At more distal regions, overlapping cellular processes with loss of junctional complexes was common, suggestive of a motile

Investigative Ophthalmology & Visual Science

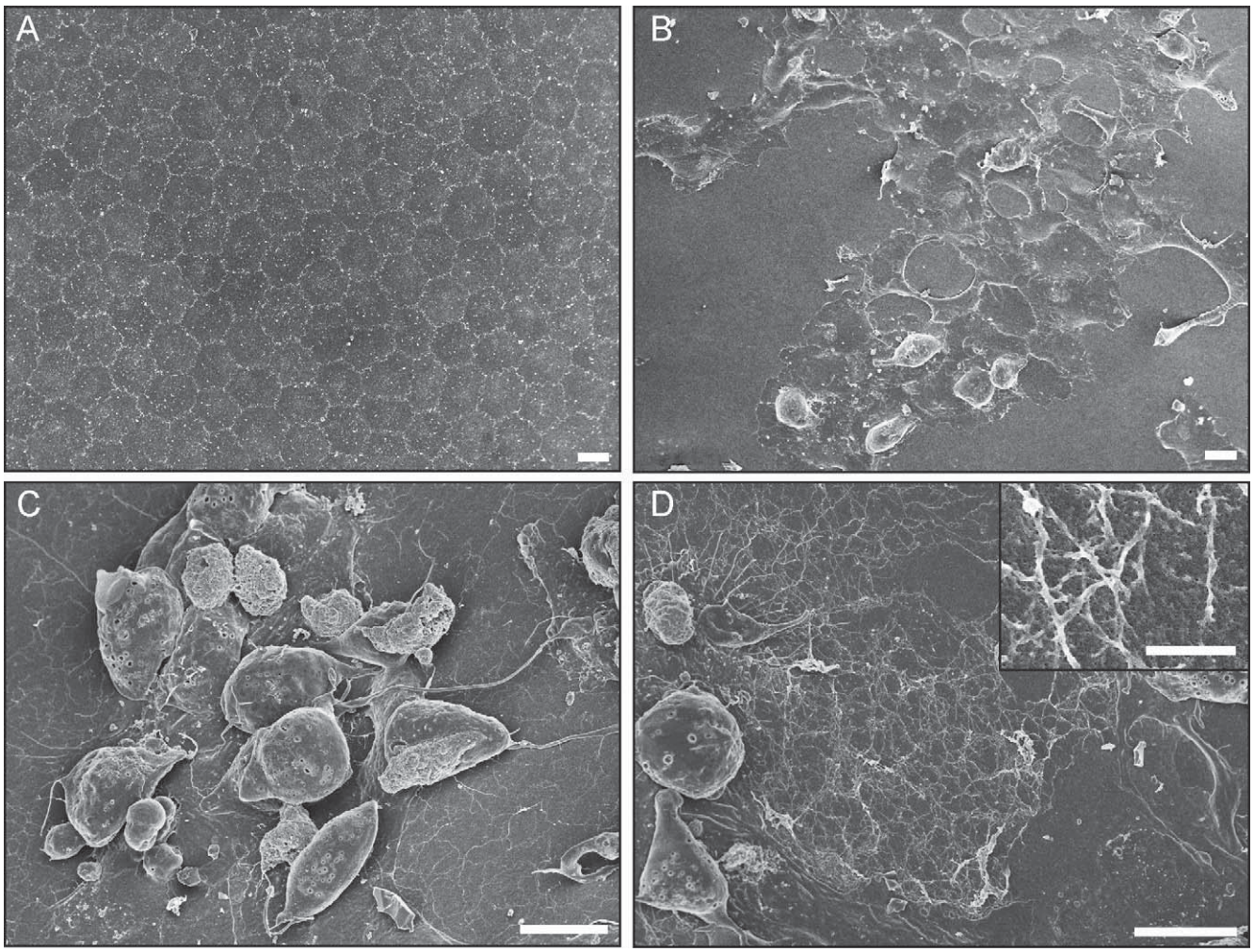

FIGURE 4. Scanning electron micrographs of the apical surface of the corneal endothelium following corneal exposure to SM vapor. (**A**) Sham-exposed control demonstrating an intact endothelial monolayer with frequent microvilli and interdigitations at regions of cell–cell contact. (**B–D**) Characteristic morphologies observed 1 day after SM exposure. The *inset* in (**D**) is a higher-magnification view of the filopodia spreading over denuded DM. *Scale bars*: 10 μm, except for the *inset*, where *scale bar*: 1 μm.

population. The rounded CEC population observed by SEM was found exclusively overlying polymorphic endothelium and displayed signs of necrosis or apoptosis.

Endothelial Disruption Is Quantitatively Characterized

In vivo confocal microscopy is a noninvasive technique that allows evaluation of CEC morphology in situ in a narrow region of the cornea. It was used to verify that postmortem evidence of endothelial injury at 24 hours was not an artifact of corneal processing. Before exposure, endothelia displayed a characteristic morphology with a regular mosaic appearance, cell density of 3219 cells/mm^2, and predominantly hexagonal shape (n = 26) (Fig. 6A). The 18 corneas that could be successfully imaged by IVM 24 hours after exposure exhibited indications of endothelial injury, with varied morphologies (Figs. 6B, 6C). In 39% (7 of 18), clusters of CECs were separated by regions of denuded DM. The remaining corneas (61% [11 of 18]) exhibited a more diffuse distribution of cell loss. Because IVM images a narrow region of the corneal endothelium, we anticipate that the variability is a consequence of whether images were captured nearer to the center or periphery of the SM lesion. Based on SEM findings, the corneas that could not be imaged may have had complete loss of endothelium in the region under examination, which would prevent IVM. Attempts to further quantify the area of CEC loss proved to be impossible due to the small field of view relative to the lesion size, limiting 1-day findings to gross descriptions of injury pattern.

The same rabbits were evaluated by IVM at 13 days to determine whether there was additional CEC loss (Figs. 6D, 6E). Among the 46% (12 of 26) of rabbits that were successfully imaged at both time points, CEC density was decreased by 29% at 24 hours ($P < 0.001$) and an additional 21% by 13 days ($P < 0.01$) (Fig. 6F). At 13 days, the CECs appeared more evenly distributed, and individual cell size seemed to have increased compared with controls, suggesting that the endothelial wound-healing response was in progress. Notably, the one resolving cornea in this cohort exhibited the most normal appearance at 13 days (Fig. 6D).

MGK and Resolved Corneas Exhibit Distinct Endothelial Morphologies

Endothelial cell morphology and structure were compared between MGK ($n = 24$) and resolved ($n = 6$) eyes 8 weeks after exposure. Resolved eyes were distinguished by the absence of

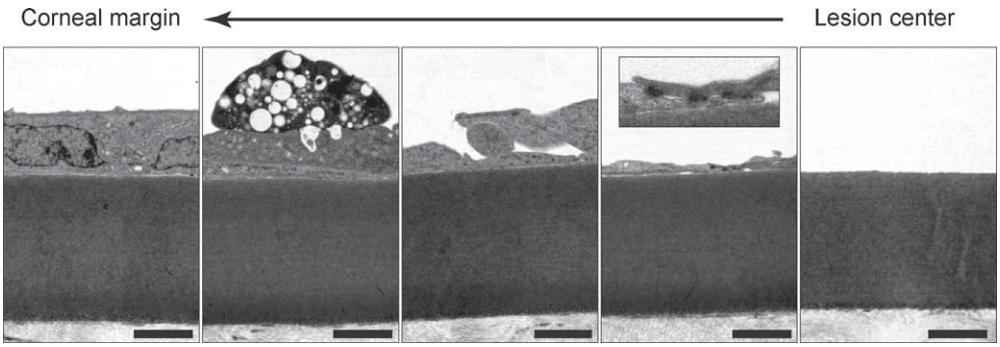

Figure 5. Transmission micrographs of corneal cross-sections demonstrating the different endothelial morphologies 1 day after corneal exposure to SM vapor. Images were taken from a single cornea but are characteristic of all corneas at 1 day. An image of the corneal margin is presented for comparison (no differences were observed compared with sham-exposed corneas). As one moves from the lesion center to the injury penumbra, denuded DM begins to exhibit an increasing density of lamellipodia. At the injury margin, overlapping cellular processes are apparent in the lesion penumbra. At the injury periphery (*second panel*), a terminally injured endothelial cell with a rounded morphology can be observed resting on at least two additional layers of endothelium. The *inset* in the *fourth panel* demonstrates tight junctions between two overlapping processes. There does not appear to be any appreciable thickening of DM across the cornea at this time point. *Scale bars*: 5 μm.

characteristic MGK sequelae during clinical evaluations such as corneal erosions, neovascularization, or corneal haze and had corneal thicknesses that were statistically indistinguishable from sham-exposed controls by 6 weeks (Supplementary Fig. S1). En face scanning micrographs of resolved eyes were strikingly similar to sham-exposed controls, with a well-organized monolayer of polygonal cells (Fig. 7A). The average CEC size was increased in resolved eyes compared with control corneas; otherwise, resolved corneas did not exhibit significant variability across the posterior surface. In contrast, MGK endothelia revealed extensive variability in cell shape and cell size among animals, indicative of a dynamic injury process (a representative montage of SEM images collected at the lesion periphery of an MGK cornea is shown in Supplementary Fig. S2). Focal variability in endothelial morphology was routinely observed in individual corneas, with some regions exhibiting enlarged but mosaic CECs and other regions displaying significant disorganization, with variable degrees of apical blebbing, areas showing denuded DM, and clearly delineated cell boundaries lacking (Figs. 7B–D). These phenomena were not observed in either resolved or naive endothelium.

As with SEM findings, TEM of resolved corneas was very similar to sham-exposed controls (Figs. 8A, 8B). In contrast, most MGK corneas exhibited diffusive thickening of the posterior DM, consistent with either edema and/or the deposition of a retrocorneal fibrous membrane (Fig. 8C).[17,18] The MGK corneas also exhibited extensive markers of CEC stress or injury, including cytoplasmic rarefication, excessive vacuolization, and swollen endoplasmic reticuli. There was a high frequency of overlapping cell processes, similar to 24-hour images and suggestive of an ongoing attempt to repopulate recently denuded DM.

Discussion

Involvement of Endothelial Toxicity in Acute and Chronic Corneal SM Injuries

Previous work has shown that SM vapor applied to the surface of the cornea penetrates to the anterior chamber within minutes, suggesting that the potential exists for endothelial toxicity.[11,19,20] Changes in corneal endothelial morphology of rabbits following SM exposure have been described using specular microscopy, and evidence of endothelial injury has been identified in human MGK corneas, including reduced CEC density with increased variability in size and morphology.[21,22] Although these findings suggest that SM injury may involve an endothelial component, the role of CEC toxicity in the pathophysiology of acute or chronic corneal SM injuries has not been evaluated to date.

Using multiple imaging methods, we found that corneal exposure to SM vapor results in an acute CEC toxicity with a centripetal injury pattern characterized by severe CEC loss at the lesion center and more diffuse CEC loss toward the injury margins. The existence of this central lesion in vivo was corroborated by IVM, and the effect of this lesion on endothelial integrity was functionally confirmed by an in vivo endothelial permeation assay. The IVM further indicated that CEC loss and endothelial disorganization persisted between 1 and 13 days, providing a potential mechanism for sustained edema beyond 2 weeks despite regeneration of an impermeant epithelial cap.[11] Although IVM offers the powerful capability of evaluating longitudinal changes in individual corneas, imaging is compromised in conditions of edema, ocular haze, and complete endothelial loss. The inability to image half of the exposed corneas at 13 days suggests that our findings may be biased in favor of the lesser-injured corneas. Regardless, the successful demonstration of confocal imaging indicates that IVM will be a valuable technique to evaluate longitudinal changes in SM-injured corneas.

Unlike the resolved corneas, which were structurally similar to sham-exposed eyes, the MGK corneas exhibited an idiotypic endothelial injury characterized by focal CEC loss, abnormal CEC morphologies, and a diffusively thickened DM. The appearance of corneal fibrosis suggests the endothelial-to-mesenchymal transition of corneal CECs, a pathological response to severe endothelial injury that involves fibroblastic transformation and deposition of atypical basement membrane components.[17,18] While we cannot discount that the endothelial toxicity observed at 8 weeks is secondary to anterior corneal degeneration, persistent epithelial lesions such as those observed during MGK generally do not have a significant effect on endothelial integrity, particularly during such a short period. Moreover, epithelial bullae, which are characteristic of severe endothelial decompensation, are an early clinical indicator of MGK onset in the vapor cup model,[14] suggesting that anterior keratopathies are a consequence of endothelial failure. Alternative mechanisms for the chronic endothelial injury include DNA:SM adducts that exert delayed genotoxic effects[23] or a subpopulation of CECs with slowly developing cytotoxic responses. We are currently characterizing longitu-

Investigative Ophthalmology & Visual Science

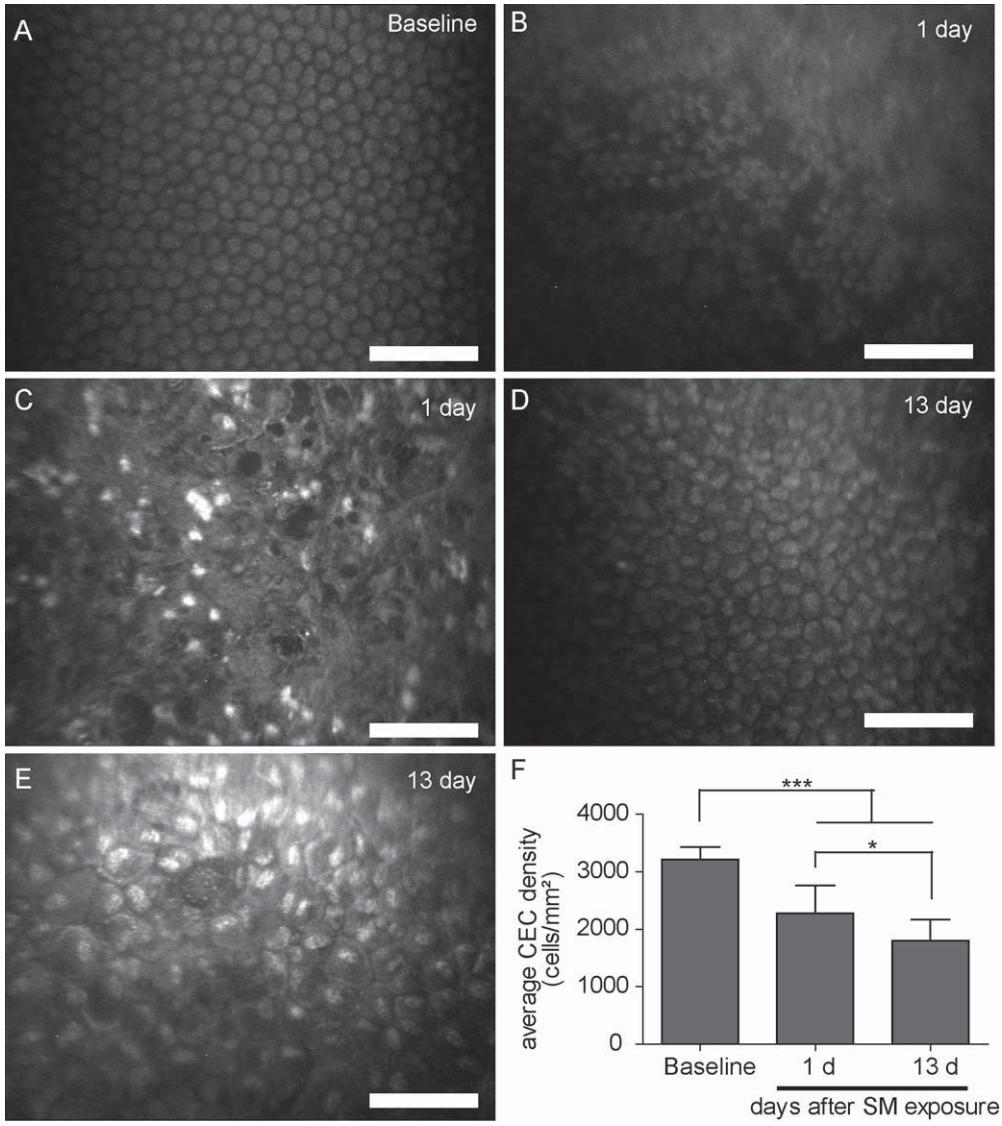

Figure 6. Representative IVM images of a cornea before (**A**) and after (**B–E**) SM exposure. (**A**) Baseline image. (**B**, **C**) Characteristic appearance 1 day after SM exposure. Note the different appearances of the endothelium. In (**C**), hyperreflective nuclei presumably result from the prominent nuclear morphology observed in Figure 4. (**D**, **E**) Endothelial morphology in corneas that would go on to resolve (**D**) or develop MGK (**E**). *Scale bars*: 100 μm. (**F**) Longitudinal changes in the average endothelial cell density (±SD) in corneas before and after exposure ($n \geq 11$ at each time point). $^{*}P < 0.05$; $^{***}P < 0.001$).

dinal changes in endothelial morphology to better understand the nature of this delayed CEC toxicity.

Implications of Endothelial Injury to the Etiopathogenesis of MGK

In the human corneal endothelium, gaps due to CEC loss are exclusively filled by spreading of proximal CECs.[24] These morphological changes compensate for endothelial loss until the barrier between the cornea and aqueous humor can no longer be maintained, resulting in persistent corneal edema and secondary anterior keratopathies.[16] Because adult human CECs do not proliferate in vivo, any loss of CECs therefore represents a permanent reduction in endothelial capacity.[24,25] Thus, while endothelial function can be restored after a mild injury by CEC spreading, more severe injuries may exceed the repair capacity of the human endothelium. Rabbits are distinct from humans in that they can undergo limited CEC proliferation, giving them an improved capacity to recover from CEC loss.[24] However, as in humans, sufficiently severe injury to the rabbit endothelium also results in irreversible corneal decompensation and secondary keratopathies.[24]

Based on these findings, we hypothesize that SM-induced endothelial failure may be the causal mechanism underlying MGK pathogenesis. This hypothesis is consistent with the dose dependence between SM and the development of MGK that has been observed in humans and rabbits, as well as the different clinical trajectories (resolved chronic MGK and delayed-onset MGK) that have been reported in human casualties.[1–3,11,12] According to this hypothesis, corneal exposure to low doses of SM results in an acute epithelial lesion, with minimal endothelial toxicity, and corneas recover without long-term complications. Alternatively, exposure to doses of SM that cause irreparable injury to the corneal endothelium would result in endothelial barrier failure, producing a persistent edema with secondary anterior keratopathies. Following a severe injury, there may be no apparent delay between the acute injury and MGK onset,

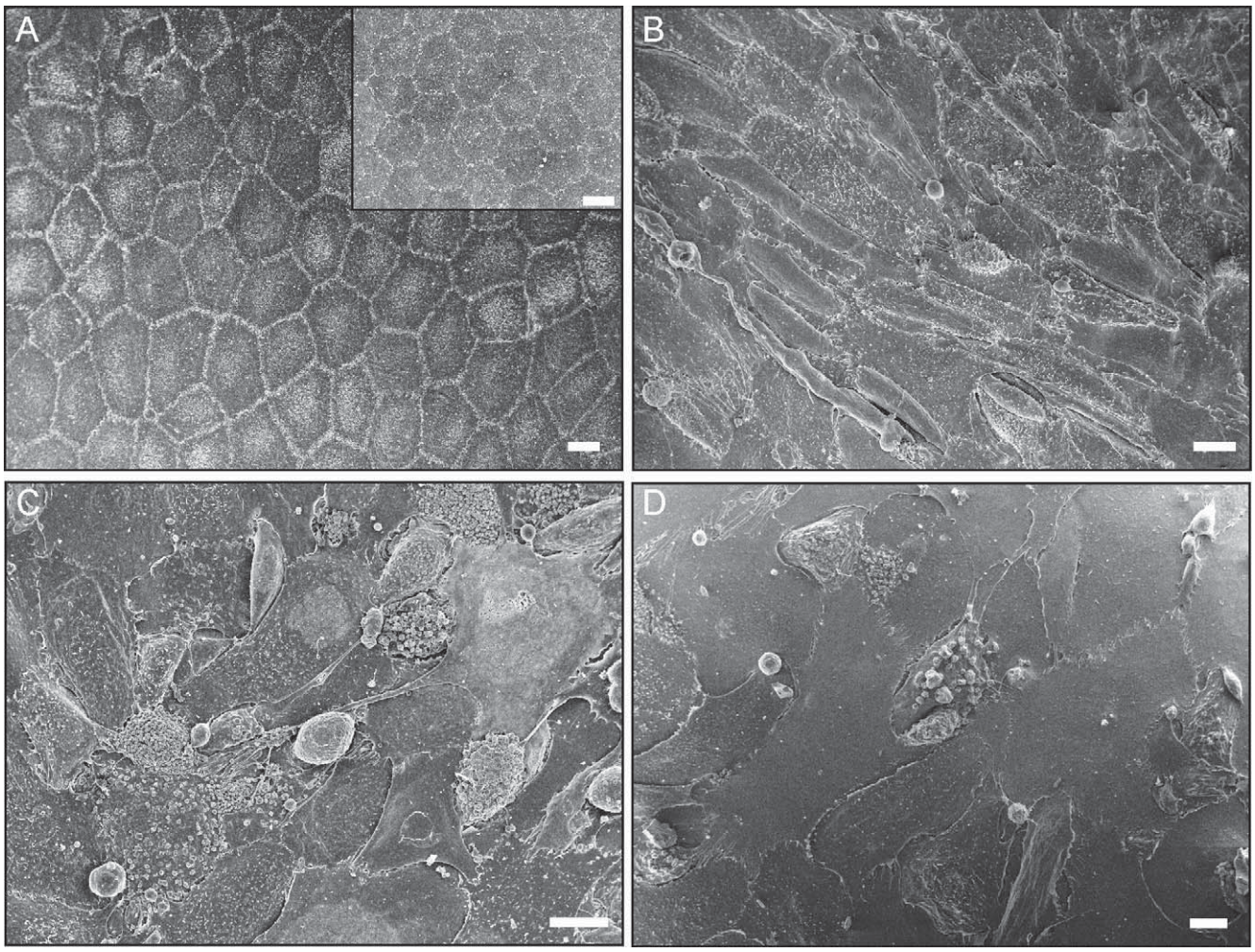

FIGURE 7. Scanning micrographs showing CEC morphologies in resolved (**A**) and MGK (**B–D**) corneas 8 weeks after SM exposure. The *inset* in (**A**) is a sham-exposed cornea at the same magnification, highlighting the increased size of CECs in resolved corneas. Note the different morphologies in (**B–D**) as described in the text, suggesting ongoing cytotoxicity and a delayed healing response. *Scale bars*: 10 μm.

resulting in the chronic clinical form of MGK. The more common delayed-onset form of MGK might be a hybrid of these two outcomes, such that endothelial barrier function is initially restored, but the subsequent loss of CECs due to age, corneal injury, and/or delayed cytotoxicity reduces CEC density below the compensation threshold, resulting in persistent edema and MGK.[26,27]

Determining the severity of endothelial injury that would be sufficient to evoke MGK in either humans or rabbits is not straightforward, in part because nonpenetrating, focal lesions in the corneal endothelium are an unusual injury modality. While charts of compensation threshold can be used to estimate the effect of cell density on the function of human endothelia, these charts have been developed from the aging-related loss of CECs and thus may not be relevant to injuries involving the focal loss of large numbers of CECs.[28] Evidence of such endothelial lesions in this study broaches the question of how the distribution of CEC loss can affect the ability of the endothelium to recover. For example, in the case of an evenly distributed loss of CECs, morphological changes in the surviving cells might rapidly allow the restoration of endothelial barrier function. In contrast, if the loss of a similar number of CECs occurred as a focal lesion, recovery may be delayed by the need for centripetal migration of surviving CECs from the lesion periphery. Consequently, in cases of sufficiently large focal lesions, the endothelial barrier may not be able to recover before the onset of irreversible secondary pathologies.

Clinical Implications of SM-Induced Corneal Endothelial Toxicity

The specific association of endothelial injury and dysfunction with MGK in both humans and rabbits has led us to hypothesize that SM-induced endothelial lesions that exceed the repair capacity of the endothelium manifest as MGK. This emphasis on endothelial injury as the etiological basis of MGK explicates the shared symptoms of the chronic and delayed-onset forms of MGK despite the different clinical time frames, provides a mechanism for sustained corneal edema despite regeneration of an impermeable corneal epithelial cap by 5 days after exposure in rabbits, and suggests that the timing of MGK onset is a function of acute CEC cytotoxicity and the subsequent rate of loss. It is also consistent with the observation that other clinical endotheliopathies involving the rapid loss of large quantities of CECs such as aphakic bullous keratopathy exhibit symptoms that are similar to MGK, including epithelial bullae, delayed limbal stem cell deficiency, and corneal inflammation.[14,29–32] For these conditions, the only effective treatment is currently corneal transplant surgery.

Investigative Ophthalmology & Visual Science

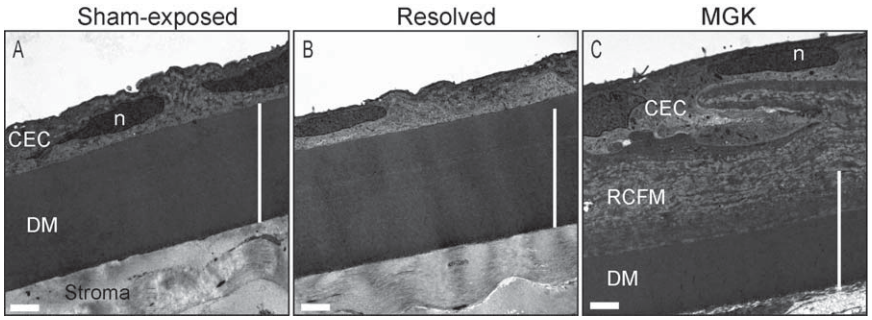

Figure 8. Transmission micrographs of a posterior cornea comparing the ultrastructure of sham-exposed (**A**), resolved (**B**), and MGK (**C**) corneas 8 weeks after SM exposure. Note the extensive thickening of the posterior unbanded DM and the formation of a retrocorneal fibrous membrane in the MGK cornea. For comparison, the *vertical white lines* represent the full thickness of DM in sham-exposed controls. n, Nucleus; RCFM, retrocorneal fibrous membrane. *Scale bars*: 2 μm.

To date, there has been little effort to characterize endothelial function in human MGK victims. Although analysis has been severely limited by the poor structural integrity of MGK corneas, histology and IVM have indicated an endothelial component to the SM injury.[22,33,34] Establishing a causal relationship between corneal pathologies and SM exposure is further complicated by the fact that human casualties are decades beyond the point of exposure. Nonetheless, the possibility of an endothelial contribution to corneal pathogenesis has important implications for SM therapeutic research. First, the failure to address an endothelial injury may explain why candidate therapies targeting the anterior cornea have had limited efficacy in preventing MGK. Second, if the extent of endothelial injury correlates with the likelihood of MGK onset, then quantitation of endothelial toxicity (e.g., by IVM) may offer a method to distinguish between eyes that will resolve and those that are at risk of developing MGK. Third, we hypothesize that early clinical interventions to restore endothelial function such as deep lamellar keratoplasty may mitigate or prevent the appearance of MGK. Given the ambiguities regarding the effect of endothelial cell proliferation on MGK onset and progression, longitudinal evaluations of CEC numbers, behavior, and morphology will be critical in studies that use the rabbit model to evaluate therapies to retain or restore the corneal endothelium. Fourth, if SM results in corneal endothelial injury, the possibility exists of toxicity to more posterior tissues at sufficiently high doses, including the retina.

Conclusions

In conclusion, we provide in vivo and postmortem evidence of corneal endothelial toxicity in acute and chronic ocular SM injuries. Based on these findings, we have synthesized a novel mechanistic explanation for the persistent edema observed in eyes that develop MGK. Endothelial injury provides a single mechanism to explicate the dose dependence of MGK onset (determined by permeation of cytotoxic quantities of SM to the endothelium), as well as the chronic and delayed-onset trajectories of MGK. This model proposes that the clinically biphasic injury progression is an epiphenomenon arising from the regenerative capacity of the corneal endothelium and hypothesizes that the probability and timing of MGK onset are functions of CEC loss. The endothelial injury suggests that therapies to restore the endothelium may mitigate the likelihood of MGK and that quantitation of endothelial loss may provide a diagnostic to identify corneas likely to develop MGK. We anticipate that these findings will motivate additional attempts to elucidate the putative pathogenic roles of endothelial injury in acute injuries and in SM survivors exhibiting chronic ocular sequelae.

Acknowledgments

The authors thank Denise Kniffen, Kim Whitten, Paula Adkins, Lindsey Devine, Susan Schulz, Riannon Hazell, and Kathy King (USAMRICD) for the sustained technical and administrative support; Cindy Kronman (USAMRICD) for editorial assistance; and the program managers at the Defense Threat Reduction Agency for their support.

Supported by the Defense Threat Reduction Agency–Joint Science and Technology Office, Medical Science and Technology Division Project CMB.CUTOC.01.12.RC.006. The authors alone are responsible for the content and writing of the paper.

This research was performed when KT and EG held Oak Ridge Institute for Science and Education (ORISE) fellowships at the United States Army Medical Research Institute of Chemical Defense (USAMRICD), administered by ORISE through an interagency agreement between the US Department of Energy and the USAMRMC.

Disclosure: **P. McNutt**, None; **K. Tuznik**, None; **M. Nelson**, None; **A. Adkins**, None; **M. Lyman**, None; **E. Glotfelty**, None; **J. Hughes**, None; **T. Hamilton**, None

References

1. Papirmeister B, Feister AJ, Robinson SI, Ford RD. *Medical Defense Against Mustard Gas: Toxic Mechanisms and Pharmacological Implications*. Boca Raton, FL: CRC Press; 1991.
2. Javadi MA, Yazdani S, Kanavi MR, et al. Long-term outcomes of penetrating keratoplasty in chronic and delayed mustard gas keratitis. *Cornea*. 2007;26:1074–1078.
3. Javadi MA, Yazdani S, Sajjadi H, et al. Chronic and delayed-onset mustard gas keratitis: report of 48 patients and review of literature. *Ophthalmology*. 2005;112:617–625.
4. Mousavi B, Soroush MR, Montazeri A. Quality of life in chemical warfare survivors with ophthalmologic injuries: the first results from Iran Chemical Warfare Victims Health Assessment Study. *Health Qual Life Outcomes*. 2009;7:2. Available at: http://www.ncbi.nlm.nih.gov/pmc/articles/PMC2647906/. Accessed September 17, 2013.
5. Khateri S, Ghanei M, Keshavarz S, Soroush M, Haines D. Incidence of lung, eye, and skin lesions as late complications in 34,000 Iranians with wartime exposure to mustard agent. *J Occup Environ Med*. 2003;45:1136–1143.

6. Richter MN, Wachtlin J, Bechrakis NE, Hoffmann F. Keratoplasty after mustard gas injury: clinical outcome and histology. *Cornea*. 2006;25:467–469.
7. Amir A, Turetz J, Chapman S, et al. Beneficial effects of topical anti-inflammatory drugs against sulfur mustard–induced ocular lesions in rabbits. *J Appl Toxicol*. 2000;20(suppl 1):S109–S114.
8. Kadar T, Dachir S, Cohen L, et al. Ocular injuries following sulfur mustard exposure: pathological mechanism and potential therapy. *Toxicology*. 2009;263:59–69.
9. Gordon MK, Desantis A, Deshmukh M, et al. Doxycycline hydrogels as a potential therapy for ocular vesicant injury. *J Ocul Pharmacol Ther*. 2010;26:407–419.
10. Babin M, Ricketts KM, Gazaway M, Lee RB, Sweeney RE, Brozetti JJ. A combination treatment for ocular sulfur mustard injury in the rabbit model. *Cutan Ocul Toxicol*. 2004;23:65–75.
11. McNutt P, Hamilton T, Nelson M, et al. Pathogenesis of acute and delayed corneal lesions after ocular exposure to sulfur mustard vapor. *Cornea*. 2012;31:280–290.
12. Milhorn D, Hamilton T, Nelson M, McNutt P. Progression of ocular sulfur mustard injury: development of a model system. *Ann N Y Acad Sci*. 2010;1194:72–80.
13. Kadar T, Turetz J, Fishbine E, Sahar R, Chapman S, Amir A. Characterization of acute and delayed ocular lesions induced by sulfur mustard in rabbits. *Curr Eye Res*. 2001;22:42–53.
14. McNutt P, Lyman M, Swartz A, et al. Architectural and biochemical expressions of mustard gas keratopathy: preclinical indicators and pathogenic mechanisms. *PLoS One*. 2012;7:e42837. Available at: http://www.ncbi.nlm.nih.gov/pmc/articles/PMC3416783/. Accessed September 17, 2013.
15. Mishima S. Corneal thickness. *Surv Ophthalmol*. 1968;13:57–96.
16. Petroll WM, Jester JV, Barry-Lane P, Cavanagh HD. Assessment of F-actin organization and apical-basal polarity during in vivo cat endothelial wound healing. *Invest Ophthalmol Vis Sci*. 1995;36:2492–2502.
17. Silbert AM, Baum JL. Origin of the retrocorneal membrane in the rabbit. *Arch Ophthalmol*. 1979;97:1141–1143.
18. Baum J. The origin of retrocorneal membranes [comment]. *Cornea*. 2000;19:124.
19. Axelrod DJ, Hamilton JG. Radio-autographic studies of the distribution of Lewisite and mustard gas in skin and eye tissues. *Am J Pathol*. 1947;23:389–411.
20. Amir A, Kadar T, Chapman S, et al. The distribution kinetics of topical ^{14}C-sulfur mustard in rabbit ocular tissues and the effect of acetylcysteine. *J Toxicol Cutan Ocul Toxicol*. 2003;22:201–214.
21. Kadar T, Cohen M, Cohen L, et al. Endothelial cell damage following sulfur mustard exposure in rabbits and its association with the delayed-onset ocular lesions. *Cutan Ocul Toxicol*. 2013;32:115–123.
22. Jafarinasab MR, Zarei-Ghanavati S, Kanavi MR, Karimian F, Soroush MR, Javadi MA. Confocal microscopy in chronic and delayed mustard gas keratopathy. *Cornea*. 2010;29:889–894.
23. Baan R, Grosse Y, Straif K, et al; WHO International Agency for Research on Cancer Monograph Working Group. A review of human carcinogens, part F: chemical agents and related occupations. *Lancet Oncol*. 2009;10:1143–1144.
24. Joyce NC, Navon SE, Roy S, Zieske JD. Expression of cell cycle–associated proteins in human and rabbit corneal endothelium in situ. *Invest Ophthalmol Vis Sci*. 1996;37:1566–1575.
25. Senoo T, Joyce NC. Cell cycle kinetics in corneal endothelium from old and young donors. *Invest Ophthalmol Vis Sci*. 2000;41:660–667.
26. Bourne WM, Nelson LR, Hodge DO. Central corneal endothelial cell changes over a ten-year period. *Invest Ophthalmol Vis Sci*. 1997;38:779–782.
27. Lopes Cardozo O. Cellular density of normal corneal endothelium. *Doc Ophthalmol*. 1979;46:201–206.
28. Wilson RS, Roper-Hall MJ. Effect of age on the endothelial cell count in the normal eye. *Br J Ophthalmol*. 1982;66:513–515.
29. Kadar T, Horwitz V, Sahar R, et al. Delayed loss of corneal epithelial stem cells in a chemical injury model associated with limbal stem cell deficiency in rabbits. *Curr Eye Res*. 2011;36:1098–1107.
30. Alomar TS, Al-Aqaba M, Gray T, Lowe J, Dua HS. Histological and confocal microscopy changes in chronic corneal edema: implications for endothelial transplantation. *Invest Ophthalmol Visual Sci*. 2011;52:8193–8207.
31. Eagle RC Jr, Laibson PR, Arentsen JJ. Epithelial abnormalities in chronic corneal edema: a histopathological study. *Trans Am Ophthalmol Soc*. 1989;87:107–124.
32. Taylor DM, Atlas BF, Romanchuk KG, Stern AL. Pseudophakic bullous keratopathy. *Ophthalmology*. 1983;90:19–24.
33. Lagali N, Fagerholm P. Delayed mustard gas keratitis: clinical course and in vivo confocal microscopy findings. *Cornea*. 2009;28:458–462.
34. Pleyer U, Sherif Z, Baatz H, Hartmann C. Delayed mustard gas keratopathy: clinical findings and confocal microscopy. *Am J Ophthalmol*. 1999;128:506–507.

Investigative Ophthalmology & Visual Science